Asian Research Journal of Mathematics

16(6): 53-69, 2020; Article no.ARJOM.56387
ISSN: 2456-477X

Analysis of a Multiscale Model of Ebola Virus Disease

Duncan O. Oganga[1*], George O. Lawi[1] and Colleta A. Okaka[1]

[1] *Department of Mathematics, Masinde Muliro University of Science and Technology, Kenya.*

Authors' contributions

This work was carried out in collaboration among all authors. DOO and GOL in collaboration designed the study, performed the mathematical analyses and wrote the first draft of the manuscript. CAO helped in the literature searches, managed the analyses of the study and sharpened presentation of the main results. All authors read and approved the final manuscript.

Article Information

DOI: 10.9734/ARJOM/2020/v16i630197
Editor(s):
(1) Dr. Sheng Zhang, Bohai University, China.
Reviewers:
(1) Sie Long Kek, Universiti Tun Hussein Onn Malaysia, Malaysia.
(2) E.Ahmed, University in Mansoura, Egypt.
(3) El Faylali Hanan, Ibn Tofail University-Morocco.
Complete Peer review History: http://www.sdiarticle4.com/review-history/56387

Original Research Article

Received: 28 February 2020
Accepted: 04 May 2020
Published: 27 May 2020

Abstract

Multiscale models are ones that link the epidemiological processes dealing with the transmission between hosts and the immunological processes dealing with the dynamics within one host. In this study, a multiscale model of Ebola Virus Disease linking epidemiological and immunological processes has been developed and analysed. The model has considered two infectious classes ; the exposed and the infected individuals. Local and global stability analyses of the Disease Free Equilibrium and the Endemic Equilibrium points of the model show that the disease dies out if the basic reproduction number $R_0^c < 1$ and persists in the population when $R_0^c > 1$ respectively. Sensitivity analysis shows that the rate of vaccination, v , is the most sensitive parameter. This indicates that effort should be directed towards implementing an effective vaccination strategy to control the spread of the disease. It has also been established that when treatment efficacy is scaled up, the viral load goes down and consequently, the transmission between hosts is also reduced. The impact of treatment on the disease spread has also been established through the coupling function $\lambda(L^*)$. The study indicates that a higher percentage of the exposed and the infected individuals should be treated to control the spread of the disease within the population.

**Corresponding author: E-mail: doganga@mmust.ac.ke;*

Keywords: Ebola virus disease; viral load; local and global stability; disease free and endemic equilibrium; sensitivity analysis; simulations.

Subject Classification: 37M05.

1 Introduction

Ebola virus disease (EVD), which is caused by Ebola virus is a rare and deadly illness whose mortality rate is high, sometimes as high as 90% [1]. It is introduced into the human population through close contact with the blood, secretions, organs or other bodily fluids of infected animals such as chimpanzees, gorillas, fruit bats, monkeys, forest antelopes and porcupines found ill or dead in the rain forest. It then spreads through human to human transmission via direct contact (through broken skin or mucous membranes) with the blood secretions, organs or other bodily fluids of infected people and with surfaces and materials such as bedding and clothing contaminated with these fluids [2].

The Characteristic symptoms of EVD which appear between 2 to 21 days include fever, joint and muscle aches, abdominal headache, sore throat, diarrhea, vomiting, stomach pains and body weakness. One week after the onset of symptoms, a rash often appears followed by hemorrhagic complications leading to death after an average of 10 days in 50 to 90% of infections [3]. Due to its deadly nature, a number of efforts are being employed to combat the disease. These include vaccination, treatment which mainly involves supportive care to maintain adequate cardiovascular function while the immune system mobilizes an adaptive response to eliminate the infection, quarantine of the infected individuals and safe burial of the infected who die.

The disease first emerged in 1976 in Sudan and Democratic Republic of Congo. The first outbreak of Ebola (Ebola-Sudan) infected over 284 people with a mortality rate of 53 %. A few months later, the second Ebola virus emerged from Yambuku, Democratic Republic of Congo (Ebola-Zaire) . It infected 318 people and it has the highest mortality rate, 88%. Other major outbreaks have been in Kikwit Congo (1995), Gulu Uganda (2000), Librevile Gabon (2000), Mbomo Congo (2002 and 2003), Luebo Congo(2007), Bundibugyo Uganda (2007) and in West Africa in Guinea, Sierra Leone and Liberia (2014) [4]. This outbreak in West Africa is the deadliest outbreak recorded in history. Currently, there is an outbreak that is going on in Democratic Republic of Congo (DRC). It was declared on 1st August 2018. As at 10th April, 2019, 1206 confirmed and probable cases had been reported during this outbreak in DRC and by 10th April 2020, confirmed cases were 3,456 and deaths were 2,276 according to World Health Organisation (WHO).

For most viral infectious diseases, there are two key processes in the host-parasite interaction. One is the epidemiological process, dealing with the disease transmission among hosts, and the other is the immunological process at the within host level [5]. Many at times, these processes are decoupled from one another.

Several Mathematical models to study EVD have been developed and analysed. These include the between host models in the references ([3],[6],[7][8],[4],[9], [10])among other studies, within host models in the references ([1],[11],[12] [13]) among others and a few multiscale models. For instance, Alexis et al. [14] developed a multiscale model of within host and between host for viral infectious diseases (can be applied to EVD). Here, the within-host model describes virus replication and the respective immune response while disease transmission is represented by a simple susceptible-infected (SI) model. The within host subsystem is given as;

$$\begin{aligned} \frac{dV}{dt} &= pV(1-\frac{V}{K_v}) - cvEV, V(0) \geq 0, \\ \frac{dE}{dt} &= (N_E - \delta_E E) + G(V)E, E(0) \geq 0. \end{aligned} \tag{1}$$

V denotes the virus, E denotes the T-Cell population, p denotes the virus replication rate and K_v denotes the carrying capacity. They imposed the following properties; $G(0) = 0$, $G'(V) = \frac{dG}{dV} > 0$ and considered a special case of G in the Michaelis-Menten form $G(V) = \frac{r_E V}{V+K_E}$ in the analysis. In this model, T- cells are replenished at a constant rate N_E and they are cleared at the rate δ_E. The virus is cleared at the rate cv while r_E and K_E denote maximum value and half saturation constant respectively.

The between host model is given below;

$$\begin{aligned} \frac{dS}{dt} &= (N_S - \delta_S S) - \beta SI, S(0) > 0, \\ \frac{dI}{dt} &= \beta SI - \delta_I I, I(0) \geq 0. \end{aligned} \tag{2}$$

where β denotes the transmission rate while δ_S and δ_S denote the death rate of susceptible individuals and infected individuals respectively. In this work, the bridge of within- to between-host was by considering transmission as a function of the viral load of the within-host level. i.e $\beta = \beta(V)$ and it has the properties $\beta(0) = 0$, $\beta'(V) > 0$. They considered three different functional forms of the coupling function including a linear, logistic and saturation function in their numerical analyses.

Their main result was the derivation of the between host model reproduction number as a general increasing function of the within host model reproduction number.

Alexis et al. [15] developed a multiscale model for EVD coupling a Susceptible Infected Recovered (SIR) between host model and a within host model considering Viral load and Antibodies. Here, they refered quite a lot to the paper [14] above.

In Amira et al. [6] , a Susceptible Exposed Infected Recovered (SEIR) model is developed in which infection is taken to spread only through interaction between the Susceptible and the infected individuals. However, it has been shown that the exposed individuals are also infectious ([16],[17]). In view of this, the model in [6] is modified by taking into consideration this reality. The new model is then coupled with a within host model (that we have developed) via the transmission rate.

2 Model Formulation

2.1 Within host model

The within host system is modeled by the following system of equations;

$$\begin{aligned} \frac{dX}{dt} &= mX(1 - \frac{X}{Q}) - (1-\rho)\beta\frac{L(t)X(t)}{1+kL(t)} - \alpha X(t), \\ \frac{dY}{dt} &= (1-\rho)\beta\frac{L(t)X(t)}{1+kL(t)} - \eta Y(t), \\ \frac{dL}{dt} &= cY(t) - \gamma L(t) \end{aligned} \tag{3}$$

where X(t), Y(t) and L(t) represents the number of uninfected target cells (Monocytes/ Macrophages and dendritic cells for the case of Ebola), infected cells and virions respectively,

m denotes growth rate of uninfected cells,
Q denotes the carrying capacity,
ρ denotes the efficacy of treatment,
β denotes the transmission rate,
k denotes the saturation constant,
α denotes the natural death rate of uninfected cells,

η denotes the death rate of infected cells,
c denotes rate of production of virions upon lysis of an infected cell,
γ denotes the death rate of virions.

2.2 Between host model

The proposed model is given by the system of Equations below;

$$\begin{aligned}
\frac{dS}{dt} &= \Lambda - \lambda SI - \lambda SqE - \mu S - vS, \\
\frac{dE}{dt} &= \lambda SI + \lambda SqE - \sigma E - \mu E, \\
\frac{dI}{dt} &= \sigma E - (\omega + \psi + \mu)I, \\
\frac{dR}{dt} &= \omega I - \mu R + vS
\end{aligned} \tag{4}$$

where
Λ denotes the rate of recruitment into susceptible population,
λ denotes the infection rate,
μ denotes the natural death rate,
v denotes the rate of vaccination,
ω denotes the recovery rate,
σ denotes the rate of transition from asymptomatic to symptomatic state,
ψ denotes the disease induced death rate,
The parameter q $(0 \leqslant q \leqslant 1)$ is a weight added to the model to emphasize the fact that a susceptible individual has a higher chance of getting infected from an infectious individual than from an exposed individual.

2.3 Multiscale model

The between host model is taken to be dependent on the value L^* which is the viral load (at equilibrium) from the within host system. This yields the system

$$\begin{aligned}
\frac{dS}{dt} &= \Lambda - \lambda(L^*)SI - \lambda(L^*)SqE - \mu S - vS, \\
\frac{dE}{dt} &= \lambda(L^*)SI + \lambda(L^*)SqE - \sigma E - \mu E, \\
\frac{dI}{dt} &= \sigma E - (\omega + \psi + \mu)I, \\
\frac{dR}{dt} &= \omega I - \mu R + vS
\end{aligned} \tag{5}$$

where $\lambda(L^*)$ is the transmission rate and is assumed to be an increasing function of L^* with $\lambda(0) = 0$ and L^* denotes the viral load at the endemic equilibrium in a single infected host. Here, $\lambda(L^*) = \frac{a(L^*)}{(L^*)+b}$ and $L^* = \frac{1}{k}[R_0^w - 1]$ where a and b denote the maximum tramsmission rate and half saturation constant of the virus respectively.

It can be shown that the model (5) is mathematically and epidemiologically well posed in the region $\Omega = \left\{ \left(S(t), E(t), I(t), R(t) \right) \in \mathbb{R}_+^4 | 0 < N(t) < \frac{\Lambda}{\mu} \right\}$ and therefore it suffices to consider it dynamically in this region.

In the model (5), the equation of the removed class is decoupled from the other three equations and so we analyse the reduced model consisting of the first three equations. This is given by

$$\begin{aligned}\frac{dS}{dt} &= \Lambda - \lambda(L^*)SI - \lambda(L^*)SqE - \mu S - vS,\\ \frac{dE}{dt} &= \lambda(L^*)SI + \lambda(L^*)SqE - \sigma E - \mu E,\\ \frac{dI}{dt} &= \sigma E - (\omega + \psi + \mu)I \end{aligned} \tag{6}$$

3 Stability Analysis of the Disease Free Equilibrium (DFE)

3.1 Reproduction number

The reproduction number for the coupled model (6), R_0^c is given by $R_0^c = \rho(FV^{-1})$ as described in Dieckmann et al. [18]

$$R_0^c = \frac{\lambda(L^*)q\Lambda}{(\sigma+\mu)(\mu+v)} + \frac{\lambda(L^*)\sigma\Lambda}{(\sigma+\mu)(\mu+v)(\omega+\psi+\mu)}. \tag{7}$$

where the Transmission matrix , F and the Transition matrix V, evaluated at the Disease Free Equilibrium (DFE) are;

$$\begin{aligned} F: &= \begin{pmatrix} \frac{\lambda(L^*)q\Lambda}{\mu+v} & \frac{\lambda(L^*)\Lambda}{\mu+v} \\ 0 & 0 \end{pmatrix}\\ V: &= \begin{pmatrix} (\sigma+\mu) & 0 \\ -\sigma & (\omega+\psi+\mu) \end{pmatrix} \end{aligned} \tag{8}$$

The first part of Equation (7) accounts for infections caused by exposed individuals while the second part is for infections caused by infected individuals. All the parameters in Equation (7) are nonnegative.

3.2 Local Stability Analysis of the Disease Free Equilibrium

The eigenvalues of the Jacobian matrix evaluated at the equilibrium gives insight into the stability properties at that equilibrium.

Theorem 3.1. *If* $R_0^c < 1$ *, then* $Z_0 = [\frac{\Lambda}{\mu+v}, 0, 0]$ *is locally asymptotically stable.*

Proof. The Jacobian matrix of model (6) is given by

$$J = \begin{pmatrix} -\lambda(L^*)I - \lambda(L^*)qE - \mu - v & -\lambda(L^*)Sq & -\lambda(L^*)S \\ \lambda(L^*)I + \lambda(L^*)qE & \lambda(L^*)Sq - \sigma - \mu & \lambda(L^*)S \\ 0 & \sigma & -(\omega+\psi+\mu) \end{pmatrix} \tag{9}$$

Evaluating Equation (9) at the DFE, we obtain;

$$J(Z_0) = \begin{pmatrix} -(\mu+v) & -\lambda(L^*)q\frac{\Lambda}{(\mu+v)} & -\lambda(L^*)\frac{\Lambda}{(\mu+v)} \\ 0 & \lambda(L^*)q\frac{\Lambda}{(\mu+v)} - \sigma - \mu & \lambda(L^*)\frac{\Lambda}{(\mu+v)} \\ 0 & \sigma & -(\omega+\psi+\mu) \end{pmatrix}$$

(10)

To investigate the stability of the DFE, we compute the eigenvalues of Equation (10).

From Equation (10),

$$\lambda = -(\mu + v) \tag{11}$$

is an eigenvalue. To determine the remaining eigenvalues, the following reduced matrix is considered;

$$J_R = \begin{pmatrix} \lambda(L^*)q\frac{\Lambda}{(\mu+v)} - \sigma - \mu & \lambda(L^*)\frac{\Lambda}{(\mu+v)} \\ \sigma & -(\omega + \psi + \mu) \end{pmatrix} \tag{12}$$

The trace of the Matrix (12) will be negative iff $\lambda(L^*)q\frac{\Lambda}{(\mu+v)} < \sigma + \mu$. That is

$$\frac{\lambda(L^*)q\Lambda}{(\mu + v)(\sigma + \mu)} < 1 \tag{13}$$

Note that the left hand side of Equation (13) is the first part of R_0^c. The determinant of Equation (12) is given by

$$DetJ_R = \left(\lambda(L^*)q\frac{\Lambda}{(\mu + v)} - \sigma - \mu\right)\left(-(\omega + \psi + \mu)\right) - \lambda(L^*)\sigma\frac{\Lambda}{(\mu + v)} \tag{14}$$

Equivalently, this is written as

$$DetJ_R = (\sigma + \mu)(\omega + \psi + \mu) - \left(\lambda(L^*)q\frac{\Lambda}{(\mu + v)}(\omega + \psi + \mu) + \frac{\lambda(L^*)\sigma\Lambda}{(\mu + v)}\right) \tag{15}$$

But using Equation (7),

$$\left(\lambda(L^*)q\frac{\Lambda}{(\mu + v)}(\omega + \psi + \mu) + \frac{\lambda(L^*)\sigma\Lambda}{(\mu + v)}\right) = (\sigma + \mu)(\omega + \psi + \mu)R_0^c \tag{16}$$

Substituting Equation (16) into Equation (15)and simplifying gives

$$DetJ_R = (\sigma + \mu)(\omega + \psi + \mu)(1 - R_0^c) \tag{17}$$

Equation (17) is positive if and only if (iff) $R_0^c < 1$. That is, the determinant is always positive whenever $R_0^c < 1$.

When $R_0^c < 1$, inequality (13) holds. We therefore conclude that the trace of J_R is negative.

The Routh Hurwitz criterion of a negative trace and a positive determinant which guarantee the existence of eigenvalues with negative real part has been met. Hence, the DFE is locally asymptotically stable whenever $R_0^c < 1$.

□

3.3 Global Stability Analysis of the Disease Free Equilibrium

To prove the global asymptotic stability, Comparison method [19] is used.

Definition 3.1. *A matrix of the form $P = \vartheta I - T$, with $T \geq 0$ (and I is an identity matrix), is said to have Z sign pattern. These are matrices whose entries off the main diagonal are negative or 0. If in addition $\vartheta \geq \rho(T)$, then P is called an M-matrix*

Lemma 3.1. *If F is nonnegative and V is nonsingular M-matrix, then* $R_0 = \rho(FV^{-1}) < 1$ *iff all the eigenvalues of (F-V) have negative real parts.*

The proof of this lemma is found in [19].

For the model (6), take $K = V - F$ and rewrite the model as

$$\begin{aligned} \frac{dx}{dt} &= -(V-F)x - \begin{pmatrix} \lambda(L^*)(S_0 - S)I + \lambda(L^*)q(S_0 - S)E \\ 0 \end{pmatrix}, \\ \frac{dS}{dt} &= \Lambda - \lambda(L^*)SI - \lambda(L^*)SqE - \mu S - vS \end{aligned} \tag{18}$$

where

$$x = \begin{pmatrix} E \\ I \end{pmatrix} \tag{19}$$

Using equation (8),

$$V - F = \begin{pmatrix} (\sigma+\mu) - \frac{\lambda(L^*)q\Lambda}{\mu+v} & \frac{-\lambda(L^*)\Lambda}{\mu+v} \\ -\sigma & \omega + \psi + \mu \end{pmatrix} \tag{20}$$

It can clearly be seen that (V-F) is a nonsingular M-matrix whenever $R_0^c < 1$. Consequently, to prove global asymptotic stability for $R_0^c < 1$, we show that $S \leq S_0$. The total population $N^* = S + E + I$ satisfies the equation

$$\frac{dN^*}{dt} = \Lambda - \mu N^* - \psi I \leq \Lambda - \mu N^* \tag{21}$$

so that $N^*(t) = S_0 - (S_0 - N^*(0))e^{-\mu t}$ with $S_0 = \frac{\Lambda}{\mu+v}$. If $N^*(0) \leq S_0$, then $S(t) \leq N^*(t) \leq S_0$ for all t. When $N^*(0) > S_0$, $N^*(t)$ decays exponentially to S_0 and either $S(t) \to S_0$ or there is some time T after which $S(t) < S_0$. Thus, from time T onwards, the function x(t) is bounded above in each component by $e^{-(t-T)(V-F)}x(T)$ which decays exponentially to 0.

4 Stability Analysis of the Endemic Equilibrium

Definition 4.1. *The endemic equilibrium state refers to the persistence of an infection within a given population.*

Theorem 4.1. *A positive endemic equilibrium point* Z^* *exists for all time* $t > 0$ *provided* $R_0^c < 1$

Proof. The positive endemic equilibrium of model (6) is given by

$$Z^* = (S^*, E^*, I^*) \tag{22}$$

To get Z^*, we equate the right hand side of model (6) to zero and solve for the state variables explicitly using elementary row operations. This gives us the following results;

$$\begin{aligned} S^* &= \frac{(\mu+\sigma)(\omega+\psi+\mu)}{\lambda(L^*)\Big(\sigma + q(\omega+\psi+\mu)\Big)}, \\ &= \frac{\Lambda}{(\mu+v)R_0^c}, \\ E^* &= \frac{\Lambda\lambda(L^*)\sigma + \Lambda q\lambda(L^*)(\omega+\psi+\mu) - (\mu+v)(\mu+\sigma)(\omega+\psi+\mu)}{\lambda(L^*)(\mu+\sigma)\Big(\sigma + q(\omega+\psi+\mu)\Big)}, \end{aligned}$$

$$
\begin{aligned}
&= \frac{1}{\lambda(L^*)(\mu+\sigma)\Big(\sigma+q(\omega+\psi+\mu)\Big)}\Big(R_0^c-1\Big),\\
I^* &= \frac{\Lambda\sigma}{(\mu+\sigma)(\omega+\psi+\mu)}-\frac{(\mu+v)\sigma}{\lambda(L^*)\Big(\sigma+q(\omega+\psi+\mu)\Big)},\\
&= \frac{\sigma(\mu+v)}{\lambda(L^*)\Big(\sigma+q(\omega+\psi+\mu)\Big)}\Big(R_0^c-1\Big) \qquad (23)
\end{aligned}
$$

Clearly from this set of three equations given by Equation (23), $E^* > 0$ and $I^* > 0$ provided $R_0^c > 1$. This ends the proof. □

4.1 Local Stability Analysis of the Endemic Equilibrium

In this section, the local stability of the Endemic Equilibrium is investigated using the lemma below.

Lemma 4.1. *A Matrix $M \in M_n(\mathbb{R})$ is stable if and only if these conditions are met: 1. The second additive compound matrix $M^{[2]}$ is stable 2. $(-1)^n det(M) > 0$*

Theorem 4.2. *If $R_0^c > 1$, then the Ebola Endemic Equilibrium point $Z^* = (S^*, E^*, I^*)$ is locally asymptotically stable.*

Proof. Note that Z^* is stable if and only if the corresponding Jacobian matrix $J(Z^*)$ is stable. $J(Z^*)$ is given by

$$
J(Z^*) = \begin{pmatrix} -\lambda(L^*)I^* - \lambda(L^*)qE^* - \mu - v & -\lambda(L^*)S^*q & -\lambda(L^*)S^* \\ \lambda(L^*)I^* + \lambda(L^*)qE^* & \lambda(L^*)S^*q - \sigma - \mu & \lambda(L^*)S^* \\ 0 & \sigma & -(\omega+\psi+\mu) \end{pmatrix} \qquad (24)
$$

and its second additive compound matrix is

$$
J(Z^*)^{[2]} = \begin{pmatrix} C & \lambda(L^*)S^* & \lambda(L^*)S^* \\ \sigma & -\lambda(L^*)I^* - \lambda(L^*)qE^* - N & -\lambda(L^*)S^*q \\ 0 & \lambda(L^*)I^* + \lambda(L^*)qE^* & \lambda S^*q - H \end{pmatrix} \qquad (25)
$$

where $C = -\lambda(L^*)I^* - \lambda(L^*)qE^* - 2\mu - v + \lambda(L^*)qS^* - \sigma, H = (\sigma+\omega+\psi+2\mu)$ and $N = (v+\omega+\psi+2\mu)$.

$Det[J(Z^*)] = C\Big[(\lambda(L^*)S^*q - \sigma - \mu)(\omega+\psi+\mu)\Big] + \Big[\Big(\lambda(L^*)^2qI^*S^* + (\lambda(L^*)^2q^2E^*S^*\Big)$

$(\omega+\psi+\mu)\Big] - \Big(\lambda(L^*)I^* + \lambda(L^*)qE^* + \mu + v\Big)\lambda(L^*)qS^* - [\lambda(L^*)]^2\sigma S^*I^* - [\lambda(L^*)]^2q\sigma S^*$ which is less than 0.

Hence the condition $(-1)^3(DetM) > 0$ of the lemma above is satisfied. This also implies that $\Sigma_1\Sigma_2\Sigma_3 < 0$ where $\Sigma_i, i = 1,2,3$ is an eigenvalue of the matrix (24). Thus, either $\mathbb{R}(\Sigma_i) < 0$ for $i = 1,2,3$ or $\mathbb{R}(\Sigma_1) < 0 \leq \mathbb{R}(\Sigma_2) \leq \mathbb{R}(\Sigma_3)$ where $\mathbb{R}(\Sigma)$ indicates the real part of Σ. The trace of matrix (24) is given by $-\lambda(L^*)I^* - \lambda(L^*)qE^* - \mu - v + \lambda(L^*)S^*q - \sigma - \mu - (\omega+\psi+\mu)$ which is less than 0 since $\lambda(L^*)S^*q < (\sigma+\mu)$. This implies that $\mathbb{R}(\Sigma_1) + \mathbb{R}(\Sigma_2) + \mathbb{R}(\Sigma_3) < 0$ and thus we

have $\mathbb{R}(\Sigma_1 + \Sigma_2) < 0$ and $\mathbb{R}(\Sigma_1 + \Sigma_2) < 0$.

The eigenvalues of the second additive compound matrix (25) are $(\Sigma_1 + \Sigma_2), (\Sigma_1 + \Sigma_3)$ and $(\Sigma_2 + \Sigma_3)$.

Using the same procedure as used above, it is established that all the eigenvalues of $J(Z^*)^{[2]}$ have negative real parts. This shows that the first part of the lemma above has been satisfied. This completes the proof. □

4.2 Global Stability Analysis of the Endemic Equilibrium

Theorem 4.3. *If $R_0^c > 1$, then $Z^* = (S^*, E^*, I^*)$ is globally asymptotically stable.*

Proof. By making change of variables and using Lyapunov method, define the function

$$Y = M^{*2} + \Pi^{*2} + O^{*2} \tag{26}$$

where

$$\begin{aligned} M^* &= S - \frac{\Lambda}{\lambda(L^*)I + \lambda(L^*)qE + \mu + v}, \\ \Pi^* &= E - \frac{\lambda(L^*)SI}{\sigma + \mu - \lambda(L^*)qS}, \\ O^* &= I - \frac{\sigma E}{\omega + \psi + \mu} \end{aligned} \tag{27}$$

Considering Equation(26), it is clear that $Y(0,0,0) = (0,0,0)$ and $Y(M,N,O) > 0$ for all (M,N,O) in the region Ω. In other words, Y is positive definite.

The derivative of Y with respect to time is given by

$$\begin{aligned} \frac{dY}{dt} &= 2\left[S - \frac{\Lambda}{\lambda(L^*)I + \lambda(L^*)qE + \mu + v}\right]\left(\frac{dS}{dt}\right) + 2\left[E - \frac{\lambda(L^*)SI}{\sigma + \mu - \lambda(L^*)qS}\right]\left(\frac{dE}{dt}\right) \\ &+ 2\left[I - \frac{\sigma E}{\omega + \psi + \mu}\right]\left(\frac{dI}{dt}\right) \end{aligned} \tag{28}$$

where $\frac{dM^*}{dt} = \frac{dS}{dt}, \frac{d\Pi^*}{dt} = \frac{dE}{dt}, \frac{dO^*}{dt} = \frac{dI}{dt}$. Substituting $\frac{dS}{dt}, \frac{dE}{dt}$ and $\frac{dI}{dt}$ with their corresponding expressions from system (6) into Equation (28) gives

$$\begin{aligned} \frac{dY}{dt} &= 2\left[S - \frac{\Lambda}{\lambda(L^*)I + \lambda(L^*)qE + \mu + v}\right]\left(\Lambda - S[\lambda(L^*)I + \lambda(L^*)qE + \mu + v]\right) \\ &+ 2\left[E - \frac{\lambda(L^*)SI}{\sigma + \mu - \lambda(L^*)qS}\right]\left(\lambda(L^*)SI - E[\sigma + \mu - \lambda(L^*)Sq]\right) \\ &+ 2\left[I - \frac{\sigma E}{\omega + \psi + \mu}\right]\left(\sigma E - I[\omega + \psi + \mu]\right) \end{aligned} \tag{29}$$

which is equivalent to

$$\begin{aligned} \frac{dY}{dt} &= -2\left[S - \frac{\Lambda}{\lambda(L^*)I + \lambda(L^*)qE + \mu + v}\right]^2\left(\lambda(L^*)I + \lambda(L^*)qE + \mu + v\right) \\ &- 2\left[E - \frac{\lambda(L^*)SI}{\sigma + \mu - \lambda(L^*)qS}\right]^2\left(\sigma + \mu - \lambda(L^*)Sq\right) \end{aligned}$$

$$
\begin{aligned}
&- 2\left[I - \frac{\sigma E}{\omega+\psi+\mu}\right]^2\left(\omega+\psi+\mu\right)\\
&< -2\left[S - \frac{\Lambda}{\lambda(L^*)I+\lambda(L^*)qE+\mu+v}\right]^2\left(\lambda(L^*)I+\lambda(L^*)qE+\mu+v\right)\\
&- 2\left[E - \frac{\lambda(L^*)SI}{\sigma+\mu-\lambda(L^*)qS}\right]^2\left(\sigma+\mu\right)\\
&- 2\left[I - \frac{\sigma E}{\omega+\psi+\mu}\right]^2\left(\omega+\psi+\mu\right) \qquad (30)
\end{aligned}
$$

Equation (30) shows that $\frac{dY}{dt}$ is negative definite.

At the point Z^* given by Equation (23), Equation (30) becomes

$$
\begin{aligned}
\frac{dY}{dt} &< -2\left[S^* - \frac{\Lambda}{\lambda(L^*)I^*+\lambda(L^*)qE^*+\mu+v}\right]^2\left(\lambda(L^*)I^*+\lambda(L^*)qE^*+\mu+v\right)\\
&- 2\left[E^* - \frac{\lambda(L^*)S^*I^*}{\sigma+\mu-\lambda(L^*)qS^*}\right]^2\left(\sigma+\mu-\lambda(L^*)qS^*\right)\\
&- 2\left[I^* - \frac{\sigma E^*}{\omega+\psi+\mu}\right]^2\left(\omega+\psi+\mu\right) \qquad (31)
\end{aligned}
$$

From Equation (31), $\frac{dY}{dt} < 0$ since S^*, E^* and I^* are all greater than 0. Therefore, the Endemic Equilibrium point Z^* is Globally asymptotically stable. □

5 Sensitivity Analysis

In this section, the sensitivity indices at the baseline parameter values are obtained. The sensitivity indices of the reproduction number are computed using Chitni's approach [20] as follows:

$$
\begin{aligned}
\Gamma_{\Lambda}^{R_0^c} &= \frac{\partial R_0^c}{\partial \Lambda}\times\frac{\Lambda}{R_0^c} = 1\\
\Gamma_{q}^{R_0^c} &= \frac{\partial R_0^c}{\partial q}\times\frac{q}{R_0^c} = 1\\
\Gamma_{\sigma}^{R_0^c} &= \frac{\partial R_0^c}{\partial \sigma}\times\frac{\sigma}{R_0^c} = \frac{\sigma\Big((\sigma+\mu)-\sigma\Big)}{q(\sigma+\mu)(\omega+\psi+\mu+\sigma)}\\
\Gamma_{\mu}^{R_0^c} &= \frac{\partial R_0^c}{\partial \mu}\times\frac{\mu}{R_0^c} = -\frac{\mu(\omega+\psi+\mu)}{\omega+\psi+\mu+\sigma} - \frac{\mu\Big[(\sigma+2\mu+v)(\omega+\psi+\mu)+(\sigma+\mu)(\mu+v)\Big]}{(\sigma+\mu)(\mu+v)(\omega+\psi+\mu)}\\
\Gamma_{v}^{R_0^c} &= \frac{\partial R_0^c}{\partial v}\times\frac{v}{R_0^c} = -\frac{v(\omega+\psi+\mu)}{(\mu+v)(\omega+\psi+\mu+\sigma)} - \frac{\sigma v}{q(\mu+v)(\omega+\psi+\mu+\sigma)}\\
\Gamma_{\psi}^{R_0^c} &= \frac{\partial R_0^c}{\partial \psi}\times\frac{\psi}{R_0^c} = \frac{-\sigma\psi}{q(\omega+\psi+\mu)(\omega+\psi+\mu+\sigma)}\\
\Gamma_{\omega}^{R_0^c} &= \frac{\partial R_0^c}{\partial \omega}\times\frac{\omega}{R_0^c} = \frac{-\sigma\omega}{q(\omega+\psi+\mu)(\omega+\psi+\mu+\sigma)}
\end{aligned}
$$

$$\Gamma_{L^*}^{R_0^c} = \frac{\partial R_0^c}{\partial L^*} \times \frac{L^*}{R_0^c} = \frac{b}{(L^*)+b}\left(\frac{q\Lambda(\omega+\psi+\mu)+\sigma\Lambda}{q\Lambda(\omega+\psi+\mu+\sigma)}\right)$$

The parameters in Table 1 are used to calculate the sensitivity indices.

Table 1. Sensitivity indices

Parameter	Value	Units	Sensitivity Index
Λ	0.6321	$peopleperday$	1
q	0.5	day^{-1}	1
μ	0.0099	day^{-1}	-0.010126956
v	0.5	day^{-1}	-1.187732576
σ	0.083	day^{-1}	0.04502415
ω	0.1	day^{-1}	-0.136334096
ψ	0.2	day^{-1}	-0.272668192
L^*	8460.054	day^{-1}	0.014150023

From the table of sensitivity index, it is clear that the reproductive number R_0^c is directly proportional to the parameters σ and L^* in that increasing each one of them increases the reproduction number. On the other hand, v, μ, ω, and ψ are inversely proportional to R_0^c. These parameters are considered more sensitive as opposed to the parameters with positive sensitivity index. Among these, the most sensitive is v (the rate of vaccination). The sensitivity index of R_0^c with respect to v is -1.187732576 implying that increasing (or decreasing) v by 10% decreases (or increases) R_0^c by 11.8773257%. This means that the enhancement of the administration of an effective Ebola virus vaccine would reduce Ebola transmission in the population.

6 Numerical Simulation and Discussion

In this section, numerical simulation is done using the parameter values given in Table 2 to explore the transmission dynamics of the model (6) with time. The results are as given by Fig. 1 to Fig. 7.

From these numerical simulations, Fig. 1 shows the stability of the DFE. It is seen that no matter the initial number of the susceptibles, the solutions converge to the point where $S_0 = \frac{\Lambda}{(\mu+v)} = 64$. This agrees with the analysis done above on the local and global stability of the DFE. In this case, the basic reproduction number is less than unity and the disease will ultimately be wiped out of the population.

The dynamics between the viral load and the number of infected individuals is depicted in Fig. 2. It is observed that as the number of virions increase, the number of infected individuals also increases upto a particular point then they begin to decrease as the number of virions remain constant. When the viral load within infected individuals increases, the average viral load in the population also increases and this affects the transmission of the disease positively. That is why there is corresponding rise in the number of infected individuals as the virions increases. However, this increase in the viral load reaches a maximum point where it cannot exceed. When that happens, we see the number of infected individuals beginning to decrease. This decrease can be attributed to the death of the Infected individuals due to high viral load.

Table 2. Parameter values for the model

Parameter	Relevant Biological Description	Units	Value	source
a	Maximum transmission rate of virus	$Mlday^{-1}$	0.0025	[15]
b	Half saturation constant of virus	day^{-1}	100	[14]
Λ	Rate of recruitment	$peopleperday$	0.6321	[17]
λ	Transmission rate	day^{-1}	0.05	varies
q	Reduced Transmission rate	day^{-1}	$(0 \leq q \leq 1)$	varies
μ	Natural death rate	day^{-1}	0.0099	[6]
v	Rate of vaccination	day^{-1}	$(0 \leq v \leq 1)$	varies
σ	Infectious rate	day^{-1}	0.083	[9]
ω	Recovery rate	day^{-1}	0.1	[7]
ψ	Disease induced death rate	day^{-1}	0.2	Assumed

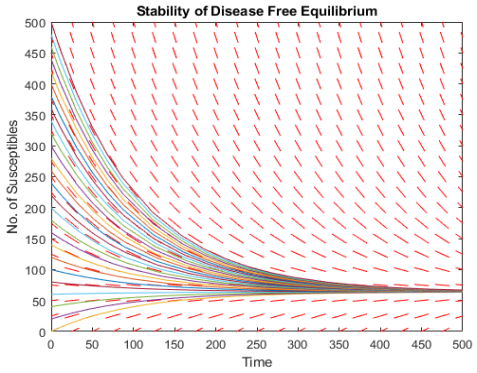

Fig. 1. The stability of DFE

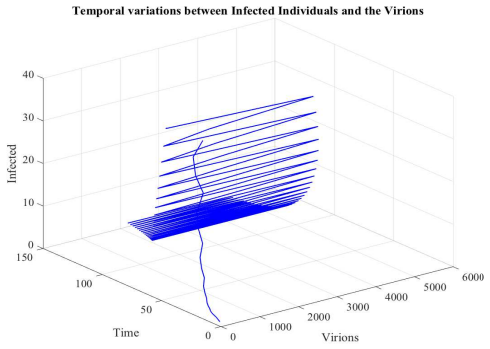

Fig. 2. Temporal variations between Virions and Infected individuals

The effect of the coupling function $\lambda(L^*)$ on the number of Exposed and the infected individuals is depicted by Figs. 3 and 4 respectively. It can be seen that as L^* increases (meaning $\lambda(L^*)$ is also increasing since $\lambda(L^*)$ is an increasing function of L^*), the number of exposed individuals and the number of infected individuals also increases respectively. At a particular value of L^*, the number of exposed individuals is always higher than the number of infected individuals. As explained earlier, this variation in the number of exposed individuals and infected individuals in the

population as L^* varies is a consequence of the variation of the average viral load in the population. This shows us that the viral load within an individual does affect the transmission dynamics of EVD between hosts. The variations in the viral load L^* used here were arrived at by varrying the efficacy of treatment ρ. It was realised that the viral load L^* and the efficacy of treatment are inversely proportional to one another. These two graphs have similar shapes because both the exposed and infected classes have infections and therefore behave in a similar manner.

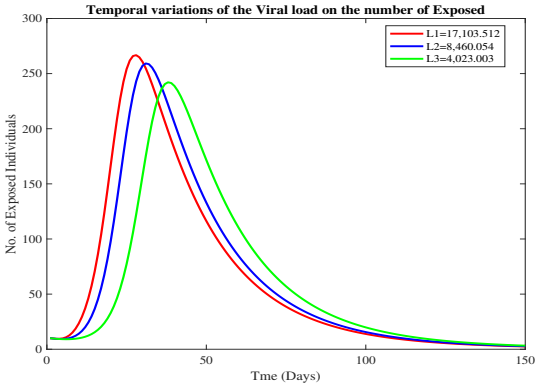

Fig. 3. Temporal variations of $\lambda(L_*)$ on Exposed Individuals

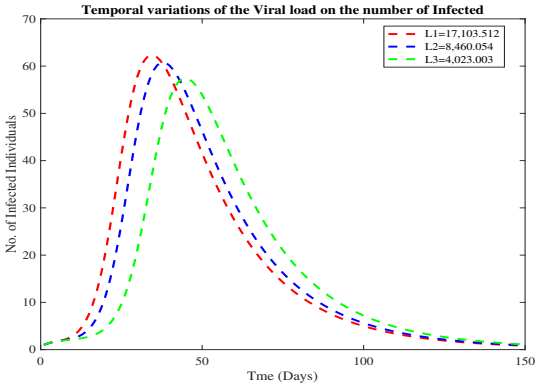

Fig. 4. Temporal variations of $\lambda(L_*)$ on Infected individuals

The effect of σ, the progression rate from exposed class to infected class, on the number of exposed individuals has been shown in Fig. 5. We see that when $\sigma = 0.5$, the number of exposed individuals rises to about 110 in day 30 and then begins to drop. However, when it is very low e.g $\sigma = 0.01$,the number of exposed individuals rises to about 350 in day 50 then begins to reduce. When σ is high, many exposed people move to the infected class within a short period of time and when σ is lower, fewer people progress to the infected class over a longer period of time. This is also illustrated by Fig. 6.

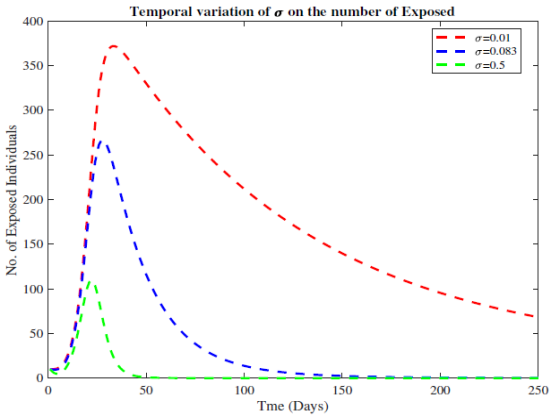

Fig. 5. Effect of σ on Exposed individuals with time

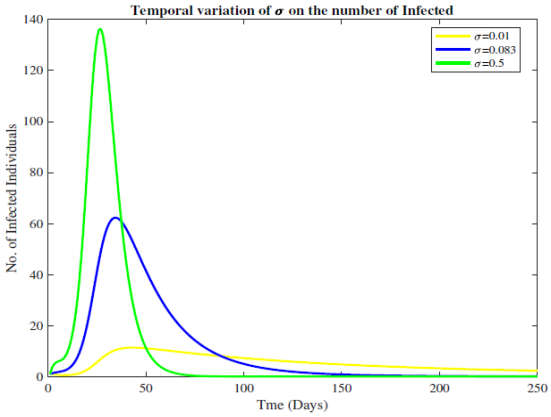

Fig. 6. Effect of σ on Infected individuals with time

The relationship between the number of exposed individuals and infected individuals is depicted by Fig. 7. It can be seen that the number of exposed individuals are always higher than the number of infected individuals. This means that the exposed (or asymptomatic) individuals contribute more infections than the symptomatic individuals. This may be due to the fact that the asymptomatic infected individuals interact freely with other healthy people since they don't show signs of Ebola virus disease as opposed to symptomatically infected individuals who are likely to be quarantied and treated. The two variables are also directly proportional to each other as can be seen on the graph. This agrees with reality since when you increase the number of infected individuals, the number of people who come into contact with them also increases.

From the foregoing discussion, we see that effort should be focussed on identifying and treating the exposed individuals. These are people who are not showing the obvious signs of EVD and yet they are infectious and from these simulations, we have seen that they are always more than the infected individuals. It will also be prudent to put in strategies to prevent the susceptible individuals from being exposed to the virus. This can be done through vaccination, quarantine, isolation and safe burials.

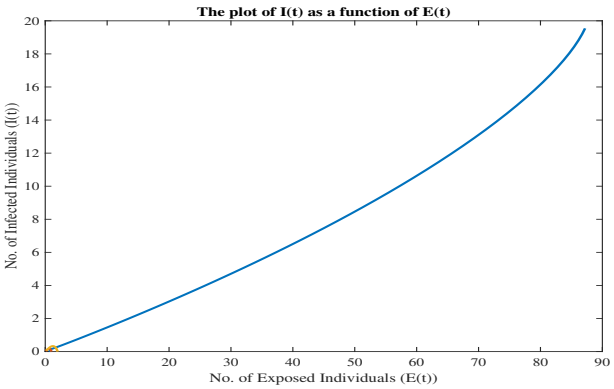

Fig. 7. Graph of I(t) as a function of E(t)

7 Conclusion

We have derived a coupled SEIR mathematical model describing EVD dynamics. This model has two infection routes, i.e infection by the Exposed Individuals and by Infected Individuals.The model has been analysed with regards to the stability of the equilibrium points. The basic reproduction number was determined and proved that the disease dies out when $R_0^c < 1$ and persists when $R_0^c > 1$. We also performed simulations where we focussed on the stability of the DFE, effect of viral load, as a result of varying efficacy of treatment, on the exposed and infected population, the effect of transfer rate σ on the number of exposed and infected individuals and the relationships between exposed and infected individuals. Sensitivity analyses of the parameters has also been done. From the analysis and numerical simulations, it has been shown that viral load, which is a within host parameter affects the between host dynamics of EVD. These results are in agreement with the study conducted by Alexis E. S Almocera and Esteban A.H Vargas [15]. Therefore we recommend that individuals be put on treatment immediately they are diagnosed with EVD to reduce the average viral load in the population. We also recommend implementation of effective mass vaccination of individuals in a susceptible population. In this study, the vaccination was considered to be 100 % effective. Further study on this can explore a vaccination strategy that is not 100% effective.

Acknowledgement

The authors acknowledge the referees for their contribution in related lines of study.

Competing Interests

Authors have declared that no competing interests exist.

References

[1] Martyushev A, Nakaoka S, Sato K, Noda T, Shingo I. Modelling Ebola virus dynamics: Implications for therapy. Antiviral Research. 2016;135:62e73. Science Direct DOI.org/10.1016/j.antiviral.2016.10.004

[2] WHO. Ebola virus disease.
Available:www.who.int/mediacenter/factsheet/fs103/en/.2016

[3] Amira R, Delfim FMT. Mathematical modelling, simulation and optimal control of the 2014 Ebola outbreak in West Africa. Hindawi Publishing Corporation; 2015.

[4] Majumder MS, Kluberg S, Santillana M, Mekaru S, Brownstein JS. Ebola outbreak: Media events track changes in observed reproductive number. PLOS Currents Outbreaks. Edition 1; 2014.
DOI:10.1371/currents.outbreaks.e6659013c1d7f11bdab6a20705d1e865

[5] Zhilan F, Jorge V, Brenda T, Maria C. A model for Coupling Within-host and Between-host Dynamics in an infectious Disease. Springer Science; 2011.
DOI;10.1007/s 11071-011-0291-0

[6] Amira R, Delfim FMT. Analysis, simulation and optimal control of a SEIR model for Ebola virus with demographic effects. Commun. Fac. Sci.Univ. Ank. Ser. A1 Math. Stat; 2017.
ISSN: 1303-5991.

[7] Durojaye MO, Ajie IJ. Mathematical model of the spread and control of Ebola virus disease. Applied Mathematics. 2017;7(2): 23-31.
DOI:10.5923/j.am.20170702.02

[8] Harout B. Modeling the spread of Ebola with SEIR and optimal control. SIAM Journal of Mathematical Analysis; 2016.

[9] Oduro FT, George A, Joseph B. Optimal control of Ebola transmission dynamics with interventions. Science Domain International. 2016;19(1):1-19. Article no. BJMCS. 29372

[10] Shen M, Yanni X, Libin R. Modelling the effects of comprehensive interventions on ebola virus transmission. Scientific Report. 2015;5:15818.
DOI:10.1038/srep 15818

[11] Sophia B, Zvi R, Mirjana P. Mathematical modeling of Ebola virus dynamics as a step towards rational vaccine design. IFMBE proceedings. 2010;32:196-200.

[12] Thomas W. Analysis and simulation of a mathematical model of Ebola virus dynamics in vivo . SIAM; 2015.

[13] Vincent M, Lisa O, Frederick G,Thi H,Tram N, Xavier L, France M, Stephan G, Jeremie G. Ebola virus dynamics in mice treated with favipiravir . Antiviral Research. 2015;123:70-77. Science Direct
DOI:10-1016/j.antiviral.2015.08.015

[14] Alexis ESA,Van KN, Esteban AHV. Multiscale model of within-host and between-host for viral infectious diseases. bioRxiv; Journal of Mathematical Biology. 2017;77:10351057.
DOI: 10.1101/174961

[15] Alexis ESA, Esteban AHV. Coupling multiscale within-host dynamics and Between-host transmission with recovery (SIR) dynamics.Elsevier; Mathematical Biosciences. 2019;309:34-41.
DOI.org/10.1016/j.mbs.2019.01.001

[16] Tae SD, Young SL. Modeling the spread of Ebola. Osong Public Health Res Perspect. 2016;7(1):43-48.
Available:http://dx.doi.org/10.1016/j.phrp.2015.12.012p
ISSN 2210-9099-ISSN 2233-6052

[17] Muhammad T, Syed IAS, Gul Z, Sher M. Ebola virus epidemic disease its modeling and stability analysis required abstain strategies. Cogent Biology. 2018;4.
DOI.org/10.1080/23312025.2018.1488511

[18] Dieckmann U, Metz J, Sabelis M, Sigmund K. Adaptive dynamics of infectious diseases: In pursuit of virulence management. New York, Cambridge University Press; 2002.

[19] James W, Van D. Further notes on the basic reproduction number. In: Brauer F, Van Den Driessche P, Wu J. (Eds) Mathematical Epidemiology. Lecture Notes in Mathematics. 2008;1945. Springer, Berlin, Heidelberg

[20] Chitnis N, Hyman J, Cushing J. Residual viremia in treated HIV+ individuals Epidemiology. PLOS Computational Biology. 2008;12:597-677.

Peer-review history:
The peer review history for this paper can be accessed here (Please copy paste the total link in your browser address bar)
http://www.sdiarticle4.com/review-history/56387